JOURNAL OF BACTERIOLOGY, Oct. 2010, p. 4973–4982 Vol. 192, No. 19
0021-9193/10/$12.00 doi:10.1128/JB.00681-10

Regulation of a Novel Gene Cluster Involved in Secondary Metabolite Production in *Streptomyces coelicolor*▽†

Hindra, Patricia Pak, and Marie A. Elliot*

Department of Biology and Institute for Infectious Disease Research, McMaster University, 1280 Main Street West, Hamilton, Ontario, L8S 4K1, Canada

Received 13 June 2010/Accepted 15 July 2010

Antibiotic biosynthesis in the streptomycetes is a complex and highly regulated process. Here, we provide evidence for the contribution of a novel genetic locus to antibiotic production in *Streptomyces coelicolor*. The overexpression of a gene cluster comprising four protein-encoding genes (*abeABCD*) and an antisense RNA-encoding gene (α-*abeA*) stimulated the production of the blue-pigmented metabolite actinorhodin on solid medium. Actinorhodin production also was enhanced by the overexpression of an adjacent gene (*abeR*) encoding a predicted *Streptomyces* antibiotic regulatory protein (SARP), while the deletion of this gene impaired actinorhodin production. We found the *abe* genes to be differentially regulated and controlled at multiple levels. Upstream of *abeA* was a promoter that directed the transcription of *abeABCD* at a low but constitutive level. The expression of *abeBCD* was, however, significantly upregulated at a time that coincided with the initiation of aerial development and the onset of secondary metabolism; this expression was activated by the binding of AbeR to four heptameric repeats upstream of a promoter within *abeA*. Expressed divergently to the *abeBCD* promoter was α-*abeA*, whose expression mirrored that of *abeBCD* but did not require activation by AbeR. Instead, α-*abeA* transcript levels were subject to negative control by the double-strand-specific RNase, RNase III.

The streptomycetes are filamentous, soil-dwelling bacteria with a complex developmental life cycle. They also have prodigious secondary metabolite production capabilities and synthesize the majority of antibiotics currently in clinical use. Secondary metabolism can be correlated with changes in morphological development, as a shift from vegetative growth to the formation of reproductive aerial structures coincides with the initiation of antibiotic production. This is coordinated at a genetic level, with mutations in many characterized developmental regulators not only affecting aerial development but also reducing or eliminating antibiotic production (10).

Streptomyces coelicolor is the best-studied streptomycete, and it serves as a model system for investigating the regulation of development and secondary metabolism (3). Conveniently, it produces two pigmented antibiotics: the red, cell-associated undecylprodigiosin and the blue, secreted actinorhodin. These pigmented metabolites have greatly facilitated genetic studies into antibiotic regulation, as changes in antibiotic levels can be readily detected by visually screening colonies on a plate (4). Antibiotic production is a tightly controlled process with many regulatory inputs, such as metabolic and nutritional status (37), small signaling molecule (γ-butyrolactone) concentrations (47), and the proposed coupling of antibiotic synthesis and resistance (27, 46). It also is subject to multiple levels of genetic regulation, including the pleiotropic regulators that affect both development and antibiotic production, global antibiotic regulators that influence the production of multiple antibiotics but do not affect development, and pathway-specific regulators that control the synthesis of a single antibiotic and often are clustered together with their target biosynthetic genes (4, 29).

Pathway-specific regulators fall into two broad classes (5): the LAL (for large ATP-binding regulators of the LuxR family) (40, 55) and the SARP (for *Streptomyces* antibiotic regulatory protein) family regulators. SARPs have an OmpR-like DNA-binding domain (49, 54), and in *S. coelicolor* they control the production of both actinorhodin (ActII-ORF4) (2) and undecylprodigiosin (RedD) (48). While all characterized SARPs appear to have roles in modulating antibiotic production, they are not limited to functioning solely within specific pathways. In fact, one of the best understood SARPs is AfsR, which is encoded at a genetic locus distinct from any secondary metabolic gene cluster, and it affects the production of at least two antibiotics in *S. coelicolor* (15). The DNA binding of AfsR has been well studied: it interacts specifically with direct, heptameric repeats (49), activating the expression of the neighboring *afsS* gene, which encodes a small, sigma-factor-like protein that affects antibiotic production via an unknown mechanism (53), and repressing the expression of genes involved in phosphate control (*phoRP* and *pstS*) (39).

In addition to transcription factor control, antibiotic production also is affected by the activity of the double-stranded RNA nuclease, RNase III. The mechanism underlying this effect is not yet understood; however, point mutations in the RNase III coding sequence, and the deletion of the gene itself (known both as *rnc* and as *absB*), abrogate antibiotic production (16, 35, 42), at least in part through the reduced expression of the pathway-specific regulators ActII-ORF4 and RedD (1).

Here, we identify a novel gene cluster that specifically affects

* Corresponding author. Mailing address: Department of Biology, McMaster University, 1280 Main Street West, Hamilton, Ontario, L8S 4K1, Canada. Phone: (905) 525-9140, ext. 24225. Fax: (905) 522-6066. E-mail: melliot@mcmaster.ca.

† Supplemental material for this article may be found at http://jb.asm.org/.

▽ Published ahead of print on 30 July 2010.

TABLE 1. Bacterial strains and plasmids used in this study

Strain or plasmid	Genotype, description, or use	Reference or source
S. coelicolor		
M600	SCP1$^-$ SCP2$^-$	8
E301	M600 Δ*SCO3287-SCO3290* (*abeABCD*)	This work
E304	M600 Δ*SCO3291* (*abeR*)	This work
J3410	M600 *rnc*::*apr*	42
E305	M600 *rnc*::*apr adpA*::*vph*	This work
E. coli		
DH5α	Plasmid construction and general subcloning	Invitrogen
ET12567/pUZ8002	Generation of methylation-free plasmid DNA	28
BW25113	Construction of cosmid-based knockouts	19
Rosetta 2(DE3)pLysS	Protein overexpression	Novagen
Plasmids/cosmids		
pIJ790	Temperature-sensitive plasmid carrying λ-RED genes	19
pIJ2925	General cloning vector	22
pWHM3	High-copy-number *E. coli*/*Streptomyces* plasmid	52
pMS82	Complementation of mutant strains	17
pET15b	Overexpression of 6× His-tagged proteins	Novagen
pMU1	Transcriptional reporter (luminescence)	12
pMC116	pWHM3 + *abeABCD* (*SCO3287-SCO3290*)	This work
pMC117	pWHM3 + α-*abeA* (α-*3287*)	This work
pMC118	pWHM3 + *abeR* (*SCO3291*)	This work
pMC119	pET15b + *abeR* (*SCO3291*)	This work
pMC120	pWHM3 + *abeABCD*, *abeR* (*SCO3287-SCO3291*)	This work
pMC122	pMS82 + *abeR* (*SCO3291*)	This work
pMC123	pIJ2925 + *abeABCD*, *abeR* (*SCO3287-SCO3291*)	This work
pMC124	pIJ2925 + *abeR* (*SCO3291*)	This work
pMC125	pIJ2925 + *abeB* (*SCO3288*)	This work
pMU1 + p*actII-4*	Reporter plasmid for *actII-orf4* expression	Y. Xu and J. Nodwell
pMU1 + p*actIII*	Reporter plasmid for *actIII* expression	Xu and Nodwell
StE15	Cosmid for *abe* gene knockouts and PCR amplification	36
2StC13	Cosmid for *adpA* knockout	36

actinorhodin production when overexpressed. We show the genes within this cluster to be differentially regulated, displaying differential expression profiles that are affected by a previously uncharacterized SARP and by RNase III.

MATERIALS AND METHODS

Bacterial strains and plasmids. *S. coelicolor* strains, *Escherichia coli* strains, and all plasmids/cosmids used in this study are summarized in Table 1. *Streptomyces* strains were grown at 30°C on solid R2YE (rich), MS (soy flour-mannitol), or SMMS (supplemented minimal) agar medium, or in liquid culture in a 1:1 tryptone soya broth (TSB)-yeast extract-malt extract (YEME) mixture, as described by Kieser et al. (24). For phenotypic comparisons of different *S. coelicolor* strains, 10^5 to 10^6 spores were streaked for single colonies on the different solid media. *E. coli* strains were grown at 37°C on solid LB medium and in liquid LB or SOB medium (38), except for *E. coli* BW25113, which was grown at 30°C when it contained the temperature-sensitive plasmid pIJ790 (19).

DNA introduction into *S. coelicolor*. DNA was introduced into *S. coelicolor* through conjugation when plasmids/cosmids carried an origin of transfer (*oriT*) or through protoplast transformation, as outlined in Kieser et al. (24).

Construction and complementation of null mutant strains. Null mutant strains were constructed using ReDirect technology (19). The knockout of the *SCO3287-SCO3290* (*abeABCD*) gene cluster, as well as *SCO3291* (*abeR*), was accomplished by gene/cluster replacement with an apramycin resistance cassette (*apr*) in cosmid StE15, followed by the introduction of the knockout cosmid into wild-type *S. coelicolor* M600 and selection for a double-crossover recombination event, as described previously (7, 14). The same process was used to knock out *adpA* in an *rnc* (also called *absB*) mutant strain, only in this case, *adpA* was replaced with a viomycin resistance cassette (*vph*) in cosmid 2StC13 (Table 1). Oligonucleotides used to generate the gene-specific disruption cassettes and to check the corresponding gene replacements are listed in Table S1 in the supplemental material. Disruption mutations were confirmed using both PCR and Southern blot analyses (data not shown). To complement the *abeR* mutant phenotype, we isolated wild-type *abeR* from pMC118 by digesting it with KpnI and HindIII (see below for details on pMC118 construction) and cloned the resulting fragment into pMS82, an integrating plasmid vector, to generate pMC122 (Table 1). This plasmid then was introduced into *E. coli* ET12567/pUZ8002 before being conjugated into the *abeR* mutant strain, *S. coelicolor* E304 (Table 1).

Construction of high-copy-number vector overexpression strains. Overexpression strains used in this study were constructed by cloning the gene(s) of interest into pWHM3 (a high-copy-number shuttle plasmid) (Table 1) and introducing the resulting recombinant plasmid into *S. coelicolor* M600 through protoplast transformation (24). The *SCO3287-SCO3291* (*abeABCD* and *abeR*) gene cluster was excised from cosmid E15 (Table 1) using KpnI, and the desired fragment was gel purified and cloned into pIJ2925 (Table 1) using a rapid DNA ligation kit (Roche) prior to transformation into subcloning-efficiency DH5α *E. coli* cells (Invitrogen). The recombinant plasmid (pMC123) was isolated and digested with BglII before the resulting *SCO3287-SCO3291*-containing fragment was subcloned into the BamHI site of pWHM3, generating pMC120. pMC120 was passaged through the nonmethylating *E. coli* strain ET12567/pUZ8002 (Table 1) prior to introduction into *S. coelicolor*. To overexpress *SCO3287-SCO3290* (*abeABCD*), this gene cluster was excised from pMC123 using BamHI, and the resulting ~4.5-kb fragment was subcloned into the BamHI site of pWHM3. The resulting construct was designated pMC116. For α-*3287* (α-*abeA*) and *SCO3291* (*abeR*) overexpression, the corresponding genes were PCR amplified with *Pfu* DNA polymerase (Stratagene) using primers OEα3287–1/OEα3287–2 and OE3291-1/OE3291-2, respectively (see Table S1 in the supplemental material). The PCR products were phosphorylated before ligation into the SmaI site of pIJ2925; the resulting clones were verified by sequencing. α-*3287* (α-*abeA*) was excised from pIJ2925 using BamHI and EcoRI, while *SCO3291* (*abeR*) was removed using BglII and EcoRI. Both fragments subsequently were cloned into BamHI and EcoRI sites of pWHM3 to give pMC117 and pMC118 as α-*abeA* and *abeR* overexpression plasmids, respectively.

Secondary metabolite assays. For the actinorhodin and undecylprodigiosin quantification of *abe*-overexpressing strains (relative to levels for empty-plasmid-

containing control strains), pregerminated spores were inoculated into R5 liquid medium (containing thiostrepton) to an optical density at 450 nm (OD_{450}) of 0.04 to 0.08. Cultures were shaken at 30°C, and samples were removed after 40, 64, 72, and 96 h. Actinorhodin and undecylprodigiosin levels then were quantified as described by Kang et al. (23). To assess the production of the calcium-dependent antibiotic (CDA), minor modifications were made to the method described by Kieser et al. (24). *S. coelicolor* spores were spread on nutrient agar plates, and these were incubated at 30°C for 24 or 48 h. Agar plugs then were excised from regions of confluent growth and were transferred from these plates into empty plugs of an equivalent size on fresh nutrient agar plates, both with and without 12 mM $CaCl_2$. These plates then were overlaid with overnight cultures of *S. aureus* ATCC 29213 diluted 1/100 in soft nutrient agar. The plates were incubated overnight at 37°C, and zones of growth inhibition were determined for strains grown on agar plates left unsupplemented or supplemented with calcium.

RNA isolation and transcript analysis. RNA isolation and Northern blot analyses were carried out as outlined by Swiercz et al. (45). Primers used for Northern blot hybridization are shown in Table S1 in the supplemental material. S1 nuclease mapping was conducted as described by Elliot et al. (14), using primers M13F and 3288R (Table S1) together with pMC125 (Table 1) as the template, to generate the probe used for mapping. For semiquantitative reverse transcription-PCR (RT-PCR), RT reactions were conducted using the SuperScript III reverse transcriptase kit (Invitrogen) according to the manufacturer's instructions, with minor modifications. Briefly, 5 μg of total RNA was mixed with RNase-free water to a final volume of 8 μl. Deoxynucleoside triphosphates (dNTPs) and gene-specific oligonucleotides were added, and the resulting mixture was incubated at 95°C for 10 min before being chilled on ice. The remaining reaction components (RNase inhibitor, reverse transcriptase, buffer, and dithiothreitol [DTT]) then were added, and reverse transcription was performed at 42°C for 50 min. The reaction was terminated by being heated at 70°C for 15 min. The resulting RT products were used as the template for subsequent PCR amplification using the following program: initial denaturation (95°C, 7 min); 15 to 28 cycles of 95°C for 45 s, 57 to 67°C for 30 s (the temperature was dependent on oligonucleotide composition, while the number of cycles was optimized to ensure amplification in the linear range of the reaction), and 72°C for 30 to 45 s (extension time was dependent on expected product sizes); and a final extension cycle of 5 min at 72°C. Negative controls (using RNA as the template) and positive controls (using chromosomal DNA or appropriate plasmid DNA as the template) were included for each PCR. PCR products were separated on a 2% agarose gel for transcript profile analyses.

***lux* reporter assays for measuring *actII-orf4* and *actIII* expression.** *Streptomyces* strains (10^5 to 10^6 spores) were grown on 0.2 ml R2YE agar plugs in 96-well flat-bottomed plates (Microfluor white plate; Thermo Scientific). Following growth for 16, 24, 32, 40, 48, 56, and 72 h, cultures were exposure to 1% decanal (luciferase substrate), and luminescence levels were determined. For each time point, 12 readings were taken (corresponding to 12 different wells/samples), and the results of three independent time courses were analyzed using the nonparametric module (Mann-Whitney test) of the SPSS v13.0 statistical analysis package to test whether luminescence levels (representing *actII-orf4* or *actIII* transcript levels) were significantly different for overexpression strains relative to those of empty-plasmid control strains.

His6-AbeR overexpression, purification, and DNA binding analyses. To analyze the DNA binding of AbeR, a His-tagged fusion protein was overexpressed and purified from *E. coli*. The *abeR* coding sequence was PCR amplified (Table S1), and the resulting product was cloned into the SmaI site of pIJ2925. This recombinant plasmid was digested with NdeI and BglII to liberate *abeR*, which then was cloned into the overexpression vector pET15b (Novagen) digested with NdeI and BamHI. The integrity of the resulting construct (pMC119) and the associated T7 promoter was confirmed by sequencing. pMC119 then was introduced into *E. coli* strain Rosetta 2 (Novagen). Protein overexpression was achieved by growing the plasmid-containing *E. coli* strains in 100 ml of LB medium supplemented with ampicillin and chloramphenicol overnight at room temperature (without isopropyl-β-D-thiogalactopyranoside induction). Cells were collected by centrifugation, and the resulting cell pellet was resuspended in lysis buffer (20 mM Tris-HCl, pH 7.5, 250 mM NaCl, 10 mM imidazole), followed by the addition of lysozyme (750 μg/ml) and protease inhibitor (Roche) per the manufacturer's instructions. The cell suspension was mechanically disrupted by sonication, after which RNase A (80 μg/ml) and DNase I (40 U; Roche) were added to the cell lysate, and the soluble fraction was separated by centrifugation. This fraction was applied to Ni-nitrilotriacetic acid agarose resin (Qiagen) before being washed three times with wash buffer (20 mM Tris-Cl, pH 7.5, 250 mM NaCl) containing increasing concentrations of imidazole (50 to 125 mM). Purified protein was eluted in wash buffer containing 250 mM imidazole and was concentrated and desalted using a Nanosep centrifugal device (Pall) with a 30-kDa cutoff. Protein concentrations were determined using a Bradford assay (Bio-Rad) (6).

FIG. 1. Genetic organization of *SCO3287-SCO3291* (the *abe* gene cluster) and the associated antisense RNA-encoding gene (α-*3287*/α-*abeA*). Transcription start sites are indicated by vertical lines, with the line widths (and associated arrows) approximating relative transcript abundance.

Electrophoretic mobility shift assays (EMSAs) were conducted using native 5% polyacrylamide gel electrophoresis. The probe was generated by PCR amplification using primers 3287–2 and 3287–3 (see Table S1 in the supplemental material), with the resulting PCR product being 5′ end labeled with [γ-^{32}P]dATP. Twenty-microliter reaction mixtures contained 0.5 nM labeled probe together with 0 to 200 nM purified protein in a buffer consisting of 10 mM Tris-HCl (pH 7.5), 150 mM NaCl, 1 mM DTT, 1 μg poly(dI-dC), and 10% glycerol. Samples were incubated at room temperature for 25 to 30 min prior to loading. Electrophoresis was performed in 1× Tris-borate-EDTA buffer at 100 V for 50 to 60 min. Gels were exposed to Kodak Biomax XAR film at room temperature for 1 h.

DNase I footprinting assays were conducted using the same binding conditions as those for the EMSA experiments. Probes were prepared by PCR amplification using 3287–2 and 3287MSAF primers (Table S1), with either 3287MSAF or 3287–2 being end labeled with [γ-^{32}P]dATP, to create probes corresponding to the coding (nontemplate) or template strands, respectively. Purified AbeR (0 to 1.6 μM) was mixed with ~6 nM probe before adding 2.5 U DNase I (Roche) for 1 min, after which PN buffer (Qiagen) was added to stop the DNase I reaction. The resulting cleavage products were purified using Qiagen MinElute columns and were eluted in 30 μl distilled H_2O. The elution products were vacuum dried for 30 to 45 min and resuspended in loading dye (80% [vol/vol] formamide; 1 mM EDTA, pH 8.0; 10 mM NaOH; 0.1% [wt/vol] bromophenol blue; 0.1% [wt/vol] xylene cyanol FF). Sequencing ladders were generated using the Sequenase v2.0 DNA sequencing kit (USB Corporation) per the manufacturer's instructions, with minor modifications. Briefly, alkaline-denatured pMC123 (Table 1) was mixed together with 5 μM the appropriate primer (3287MSAF/3287–2; see Table S1 in the supplemental material) in a total volume of 10 μl. These mixtures then were boiled for 3 min and placed immediately on ice for 5 min before being centrifuged for 30 s. To each tube, buffer, DTT, [α-^{33}P]dATP, and Sequenase were added per the manufacturer's instructions, and the resulting reaction mixtures were mixed with the dGTP labeling mix and the ddG/A/T/C termination mix, which previously had been warmed to 37°C. These mixtures were incubated at 37°C for 2 min before stop solution was added (USB Corporation). All samples (reaction and sequencing) were heated at 90°C for 3 to 5 min prior to being loaded onto a 6% denaturing polyacrylamide gel, which was run at 45 W for either 45 (template strand) or 75 min (coding/nontemplate strand).

RESULTS

Bioinformatic analysis of the *SCO3287-SCO3291* genetic region. Our interest in this genetic region originally was stimulated by the presence of an antisense RNA, encoded by α-*3287* on the strand opposite *SCO3287* (45). *SCO3287* is the first gene of an apparent four-gene operon that is, to date, unique to *S. coelicolor* and its very close relative, *S. lividans* (Fig. 1). *SCO3287* encodes a highly charged (arginine-rich) cytoplasmic protein of 172 amino acids (aa). It is devoid of obvious functional motifs and bears no sequence similarity to any known protein. It is followed by two predicted membrane protein-encoding genes, *SCO3288* and *SCO3289*, whose products are 243 and 536 aa, respectively. Neither of these genes is similar to any characterized gene, although *SCO3289* encodes a product with homologues in other *Streptomyces* species, notably *S. avermitilis*, where it is cotranscribed with a smaller downstream

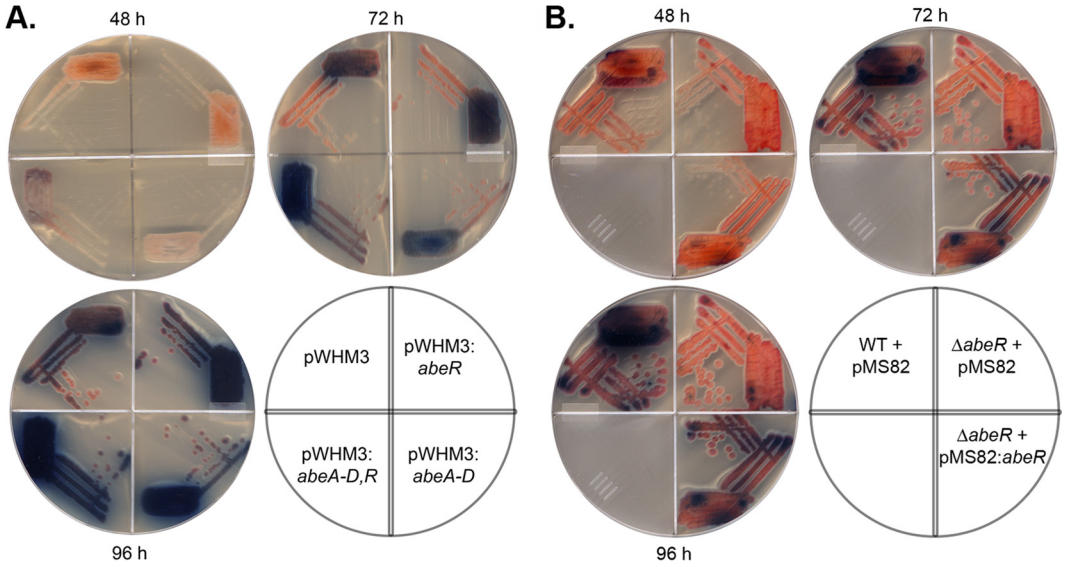

FIG. 2. Phenotypic effects of *abe* gene overexpression and *abeR* deletion during growth on rich R2YE agar medium. (A) Wild-type *S. coelicolor* (M600) containing the high-copy-number plasmid pWHM3 alone or carrying *abeABCD* (*SCO3287-SCO3290*), *abeR* (*SCO3291*), or both *abeABCD* and *abeR*, grown for 2 to 4 days. (B) Comparison of wild-type (M600) and *abeR* deletion strains carrying the empty integrating (single-copy) plasmid vector pMS82, with the *abeR* mutant strain carrying a wild-type copy of *abeR* in pMS82. To best visualize antibiotic production, all pictures were taken from the underside of the plates, and to ensure reproducibility, experiments were repeated at least four times using a minimum of two independent spore stocks as the inoculum.

gene, and *S. griseus*, where it exists as a single genetic unit. In *S. coelicolor*, *SCO3289* appears to be translationally coupled with *SCO3290*, which encodes a 249-aa cytoplasmic protein with a predicted nucleotide binding domain similar to the Toll/interleukin-1 receptor (TIR-like) domain, suggesting a possible role in signal transduction (30) or protein-protein interactions (44).

Downstream of this four-gene cluster, oriented in the same direction, is a predicted transcription factor-encoding gene. Its product, SCO3291, is 477 aa, with a multidomain architecture. The C terminus of SCO3291 shares similarity with conserved hypothetical proteins from a wide variety of bacteria, although these are largely single-domain proteins. The function of this C-terminal region is unknown; it is worth noting that proteins with this domain usually are encoded adjacent to genes whose products have TIR-like domains, such as that found in SCO3290. The N terminus of SCO3291 contains an OmpR-like DNA binding domain (31) and a so-called BTAD, or bacterial transcription activator domain (58). These two domains are common to all SARP family regulators (54, 58) and suggest that SCO3291 has DNA binding properties. While many SARPs are encoded within antibiotic biosynthetic gene clusters and act as pathway-specific antibiotic regulators, the target genes for SCO3291 are not immediately obvious, as the nearest secondary metabolic gene cluster is 38 kb away (the calcium-dependent antibiotic cluster).

Actinorhodin production increases upon gene/gene cluster overexpression. To address the biological role of the *SCO3287-SCO3290* gene products and the function of SCO3291, we first replaced the four-gene cluster with an antibiotic resistance gene and compared its phenotype to that of wild-type *S. coelicolor*. Both colony development and antibiotic production by the mutant strain closely resembled that of its wild-type parent when grown on a variety of solid culture media (data not shown). In contrast, the overexpression of *SCO3287-SCO3290* (on a multicopy plasmid) significantly increased actinorhodin production during growth on solid rich (R2YE) (Fig. 2A) and supplemented minimal (SMMS) media (data not shown); CDA production was unaffected (data not shown). Increased antibiotic production could be due to the overexpression of the four-gene cluster itself or could result from the increased expression of the antisense RNA, α-*3287*, encoded on the strand opposite *SCO3287* (Fig. 1). To differentiate between these two possibilities, we created an α-*3287* overexpression strain by introducing α-*3287* on a multicopy plasmid vector into wild-type *S. coelicolor*, and we found that this strain produced antibiotics at a level equivalent to that of an empty-plasmid control strain (data not shown). This suggested that the enhanced actinorhodin production seen for the *SCO3287-SCO3290* overexpression strain was due to the overexpression of one or more of the four protein-encoding genes and not α-*3287*. Given the ability of these gene products to modulate antibiotic levels, we propose that *SCO3287-SCO3290* be renamed *abeABCD* for antibiotic enhancement upon overexpression, and that α-*3287* be renamed α-*abeA*.

We used a similar approach to investigate the role of SCO3291 in *S. coelicolor* development and metabolism, creating both *SCO3291* deletion and overexpression strains. The replacement of *SCO3291* with an apramycin resistance gene resulted in decreased actinorhodin production relative to that of its wild-type parent (Fig. 2B); this defect could be reversed upon complementation with a wild-type copy of *SCO3291* on the integrating plasmid vector pMS82 (Fig. 2B). In contrast, overexpressing *SCO3291* either on its own or with *abeABCD* resulted in increased actinorhodin production compared to that of empty-plasmid-containing control strains (Fig. 2A). We

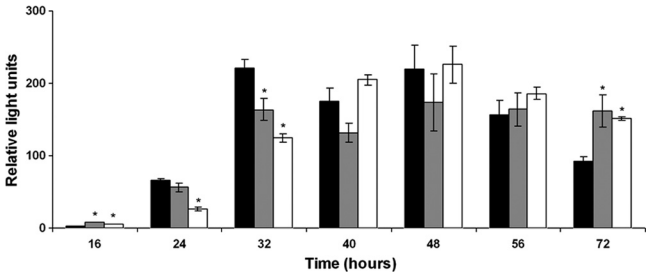

FIG. 3. Expression of *actII-ORF4* as measured using the *lux* reporter system during a 72-h time course. Luminescence levels are shown as relative light units (*y* axis). Black bar, wild-type *S. coelicolor* containing the high-copy-number plasmid pWHM3; gray bar, wild-type strain containing pWHM3+*abeR*; white bar, wild-type strain containing pWHM3+*abeABCD*. All strains carried a chromosomally integrated pMU1 reporter plasmid containing the *actII-orf4* promoter cloned upstream of the *lux* genes. Strains were grown on R2YE agar plugs in 96-well plates. Luminescence levels reflect the means (± standard errors) from three independent experiments following the subtraction of background levels (luminescence of each strain carrying pMU1 alone). Asterisks indicate those samples in which the mean luminescence levels were significantly different (at a 95% confidence level) between *abe* overexpression and plasmid-alone (pWHM3)-containing strains.

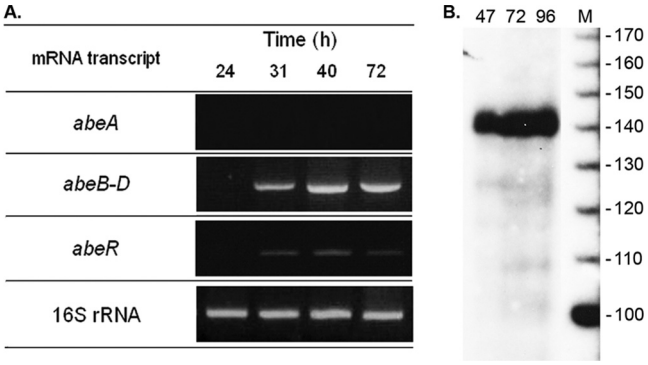

FIG. 4. Expression profiles for *abeA*, *abeBCD*, and *abeR* during growth on rich R2YE agar medium. (A) Semiquantitative RT-PCR using RNA samples harvested from wild-type *S. coelicolor* (M600), with the number of PCR amplification cycles having been optimized for each transcript (*abeA*, 27 cycles; *abeBCD*, 25 cycles; *abeR*, 28 cycles; and the 16S rRNA gene, 15 cycles). 16S rRNA served as a positive control for the RT and PCR and also as a control for RNA levels. (B) S1 nuclease mapping of the 5′ end of the *abeBCD* transcript. RNA samples were harvested from the *abeABCD* overexpression strain (Table 1) after 47, 72, and 96 h of growth and were run adjacent to a 10-bp ladder (M).

therefore propose that *SCO3291* be renamed *abeR*, given the effect of its overexpression on antibiotic production.

We also monitored the actinorhodin and undecylprodigiosin levels for *abeABCD*, *abeR*, and *abeABCD* and *abeR* overexpression strains relative to those for a control plasmid-containing strain during liquid culture growth. We observed no difference in the level of undecylprodigiosin produced by the overexpression and control strains (data not shown), and while we did observe increased actinorhodin production for the overexpression strains on some occasions, this effect was not consistently reproducible (data not shown), unlike the increased actinorhodin production that was observed consistently for overexpression strains grown on solid culture (Fig. 2).

Enhanced actinorhodin production by overexpression strains may be due to the extended expression of *actII-orf4* but not to an overall increase in expression. Many characterized antibiotic regulators mediate their effects through the transcriptional control of pathway-specific activators (1, 33, 37). As actinorhodin levels were significantly increased in both *abeABCD* and *abeR* overexpression strains during growth on solid media, we sought to probe the effect of this overexpression on the transcription of the actinorhodin pathway-specific regulator *actII-orf4*, and the actinorhodin biosynthetic gene *actIII*, using luciferase transcriptional reporters (12). We introduced the reporter constructs and corresponding control plasmid into the *abeABCD* and *abeR* overexpression strains and monitored luminescence levels over time. We did not detect any consistent differences in *actIII* expression during the 3-day time course (data not shown). For *actII-orf4*, however, expression from 24 to 32 h actually was lower in the two overexpression strains than in the control strain, but by 72 h we observed a statistically significant increase in promoter activity in both overexpression strains compared to that of the wild type (Fig. 3), suggesting that the extended expression of *actII-orf4* contributes to enhanced actinorhodin production.

Transcription analyses of *abeABCD* reveal a complex operon expression structure. To begin dissecting the function of the unique *abe* gene cluster, we examined the expression of these genes on rich (R2YE) medium, starting with *abeA*. Unexpectedly, we could not detect *abeA* transcripts at any point during a 3-day time course using semiquantitative RT-PCR (Fig. 4A). When we looked at the expression of *abeBCD*, however, transcripts were readily detectable; these genes were expressed first during the onset of secondary metabolism and aerial hyphae formation (at 31 h), and expression continued through at least 72 h (Fig. 4A). This suggested that despite being separated from *abeA* by a mere 8 bp, *abeBCD* was transcribed independently. To further explore this possibility, S1 nuclease mapping was conducted using a probe that encompassed the final 326 nucleotides (nt) of the *abeA* coding sequence and the first 64 nt of the *abeB* coding sequence. We identified a transcription start site ~77 nt upstream of the *abeB* translation start site within *abeA* (Fig. 4B) and 210 nt downstream of the α-*abeA* transcription start site (Fig. 1 and 5E).

To further examine *abeA* expression and determine whether *abeBCD* expression was completely uncoupled from that of *abeA*, we investigated the transcription of these genes in our *abeABCD* overexpression strain, where the gene cluster was cloned into a high-copy-number plasmid. We found *abeA* to be constitutively expressed and determined that there was transcriptional read-through into *abeB* (and likely *abeCD*), as determined by RT-PCR using primers that flanked either side of the *abeBCD*-specific promoter within *abeA* (see Fig. S1 in the supplemental material). Taken together, these findings suggest that *abeABCD* is constitutively transcribed at a low level, while *abeBCD* is expressed at much higher levels and is induced at a time corresponding to the initiation of antibiotic production and aerial hyphae formation.

AbeR activates the expression of *abeBCD*. We also examined the expression of *abeR* and found the timing of its expression to be very similar to that of *abeBCD* in a wild-type background,

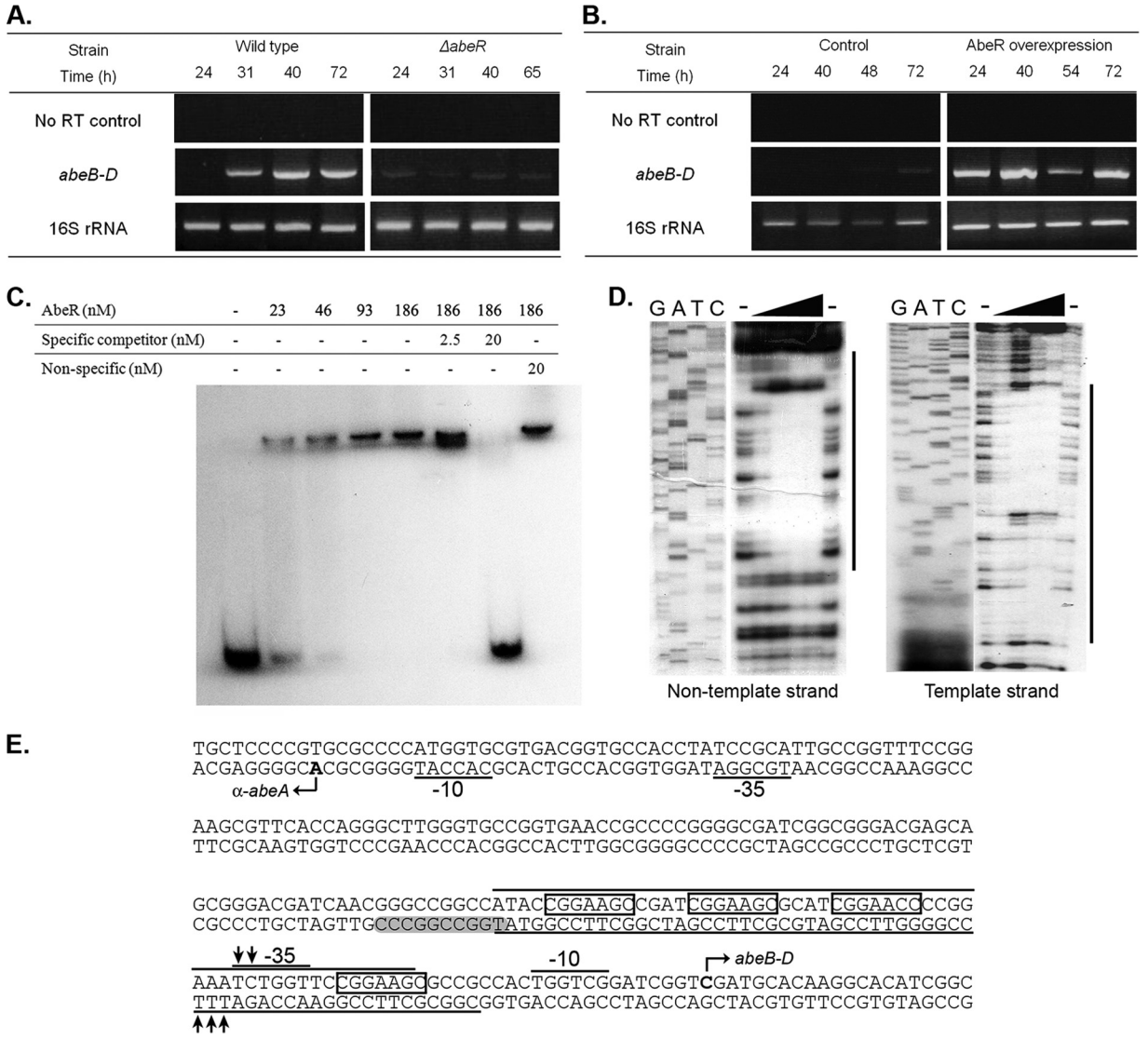

FIG. 5. Regulation of *abeBCD* transcription by AbeR. Shown are transcription profiles of *abeBCD* in *S. coelicolor* wild-type and *abeR* deletion strains (A) and in *abeR* overexpression and plasmid (pWHM3)-alone control strains (B), as determined using semiquantitative RT-PCR. RNA samples used in the RT-PCR were harvested at time points indicated above each panel; the number of PCR amplification cycles was optimized for each experiment: 25 cycles (A) and 27 cycles (B) (note that strains carrying the high-copy-number plasmid pWHM3 appear to have reduced overall transcript levels compared to those of non-plasmid-containing strains [unpublished data]). For the no-RT control PCR, RNA (not subjected to reverse transcriptase) served as the template to ensure no DNA contamination. The 16S rRNA gene was amplified (15 cycles) as a control for RNA levels and RNA integrity. (C) EMSA of [γ-^{32}P]dATP-radiolabeled probe (214 bp) containing the *abeBCD* promoter region together with His_6-AbeR. AbeR binding specificity was tested using specific (cold probe) and nonspecific competitor DNA (*chpD* coding sequence). (D) DNase I footprinting assay of His_6-AbeR binding to the *abeBCD* promoter region. Protected regions are indicated by the vertical lines to the right of each footprint. Increasing concentrations of purified AbeR (0 to 1.67 μM, with increasing concentrations of protein indicated by the black triangle) were incubated together with 6 nM singly end-labeled probe. Sequencing ladders are shown to the left of each footprint. (E) Coding sequence of *abeA* encompassing the approximate -10 and -35 promoter sequences of α-*abeA* and *abeBCD*. Mapped transcriptional start sites for both transcripts are designated by boldface letters. DNA sequences protected by AbeR are indicated by horizontal lines, and the protected four direct heptameric repeats are boxed. Sites of DNase I hypersensitivity are indicated by vertical arrows, while a potential AdpA binding site is shaded in gray.

with transcripts detected from 31 to 72 h (Fig. 4A). Given this finding and considering that the overexpression of *abeR* had phenotypic consequences similar to those of the overexpression of *abeABCD*, we wondered whether there might be a regulatory connection between AbeR and *abeBCD*. To probe this possibility, we examined the transcript levels of *abeBCD* in the *abeR* deletion and overexpression strains described above. We found that *abeBCD* expression was barely detectable in the *abeR* deletion strain (Fig. 5A), while in the overexpression strain, transcript levels were increased considerably compared to those of an empty-plasmid-carrying control strain (Fig. 5B). We also tested whether *abeA* transcripts were detectable in the *abeR* overexpression strain, but as was the case for the wild type, no expression could be observed (data not shown).

To determine whether AbeR was directly involved in controlling *abeBCD* expression, we overexpressed AbeR as an

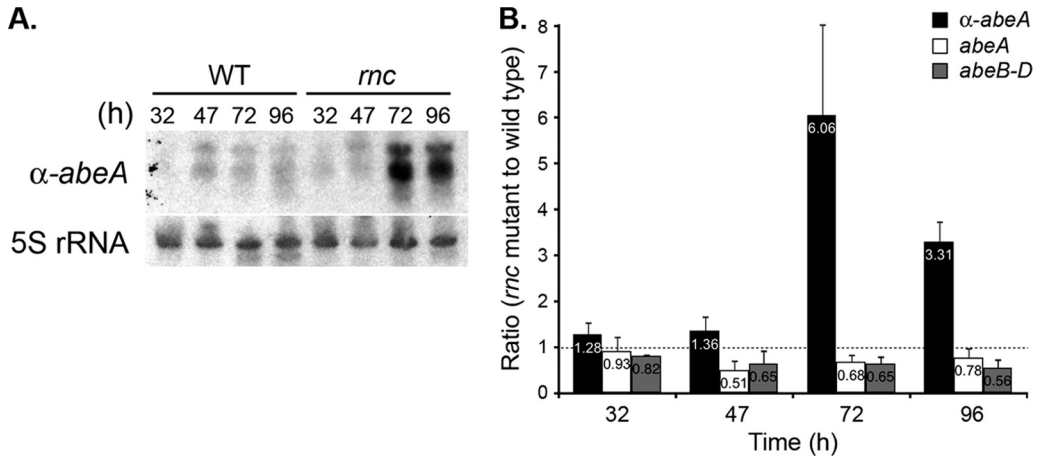

FIG. 6. Expression of α-*abeA*, *abeA*, and *abeBCD* in *S. coelicolor* wild-type and mutant strains lacking RNase III. (A) Northern blot analysis of α-*abeA* expression in wild-type and *rnc* (*absB*) mutant strains carrying the *abeABCD* overexpression plasmid (pMC116; Table 1). 5S rRNA was examined as a control for RNA integrity and loading. (B) Levels of α-*abeA*, *abeA*, and *abeBCD* in the *rnc* (*absB*) mutant strain relative to its wild-type parent *S. coelicolor* M600. Transcript levels were normalized relative to 5S rRNA (for α-*abeA*) and 16S rRNA genes (for *abeA* and *abeBCD*) to account for differences in input template RNA and *tsr* levels to account for differences in plasmid copy number levels for wild-type and mutant strains. Transcript abundance was determined using the ImageJ analysis of Northern blotting (α-*abeA*) and RT-PCR (*abeA*, *abeBCD*, 16S rRNA gene, *tsr*) results. The data presented are the averages (± standard deviations) from four experiments (two experimental replicates of two independent RNA time courses).

N-terminally His-tagged protein in *E. coli* for use in EMSAs, and we purified this protein using Ni affinity chromatography. EMSAs were performed using a DNA fragment that encompassed both the α-*abeA* (antisense gene) and *abeBCD* promoter regions as the probe. We found this fragment to be effectively bound by the AbeR fusion protein at a concentration of 93 nM. Competition experiments confirmed the specificity of this interaction, with cold probe effectively competing with the labeled probe for binding, but an unrelated DNA fragment (the *S. coelicolor chpD* coding sequence, where ChpD is associated with aerial development but not antibiotic production [14]) failed to compete (Fig. 5C). The analysis of the sequence contained within the specifically bound DNA fragment revealed there to be four tandemly arranged direct repeats of 7 nt, with the first three repeats each separated by 4 nt and the fourth located a further 15 nt downstream. DNase I footprinting experiments were conducted to determine whether these repeated regions were protected by AbeR binding. As seen in Fig. 5D and E, protection by AbeR covered the repeated regions, with sites of DNase I hypersensitivity seen on both strands within the 15-bp region separating the third and fourth repeats.

AbeR does not control α-*abeA* expression. As the binding site of AbeR was located between the promoter regions for *abeBCD* and α-*abeA*, we wanted to determine whether AbeR also affected the expression of α-*abeA*. Using Northern blotting, we examined α-*abeA* transcript levels in the *abeR* overexpression and deletion strains and found its expression to be unaffected in each instance (data not shown), suggesting that the effect of AbeR binding was limited to the activation of *abeBCD* expression.

RNase III contributes to the destabilization of α-*abeA* transcripts. Having established that AbeR played an important role in activating the expression of *abeBCD* but did not impact α-*abeA* expression, we wanted to identify factors that affected α-*abeA* expression, as its expression profile mirrored that of *abeBCD* and *abeR* (Fig. 6A) (45). The positioning of α-*abeA* suggested that the most likely interaction partner for α-*abeA* would be *abeA*-containing transcripts, and the resulting double-stranded RNA complexes would be reasonable targets for RNase III. We therefore examined the expression of α-*abeA* in wild-type and RNase III (*rnc* [*absB*]) mutant strains carrying the *abeABCD* overexpression construct. We found that α-*abeA* transcripts were present in far greater abundance during later stages of growth (3 to 4 days) in the *rnc* (*absB*) mutant strain than in the wild type (Fig. 6A), suggesting that α-*abeA* may be targeted for degradation by RNase III late in development, possibly in conjunction with its predicted target, *abeA*. However, when we examined *abeA* expression, expecting to see similarly increased levels in the *rnc* (*absB*) mutant, we found this was not the case. After normalizing *abeA* transcript levels using the 16S rRNA transcript control, and accounting for plasmid copy number using transcript levels of the plasmid-carried *tsr* (thiostrepton resistance) gene, we found there to be less *abeA* expression at all time points in the *rnc* (*absB*) mutant than with the wild-type strain (Fig. 6B). Similar effects were observed for *abeBCD* transcript levels (Fig. 6B). No obvious correlations could be drawn between α-*abeA* and *abeA* expression levels, suggesting that despite being perfectly complementary, α-*abeA* had little effect on *abeA* transcript stability.

The RNase III-dependent destabilization of α-*abeA* is independent of AdpA activity. The change in α-*abeA* transcript levels in the *rnc* (*absB*) mutant compared to that of its corresponding wild-type parent was reminiscent of that observed for *sti1* (*SCO0762*) and *ramR*, whose expression also was upregulated later in development in an *rnc* (*absB*) mutant (21). Recent work has shown this upregulation to be indirect, resulting not from the reduced cleavage of these mRNAs by RNase III but from increased AdpA-dependent activation (56). AdpA is a pleiotropic regulator (25, 32), and its transcripts are targeted

for degradation by RNase III; the loss of RNase III leads to increased AdpA levels and, correspondingly, increased transcription of AdpA-activated genes (56). We examined the sequence upstream of α-*abeA* and found a reasonable match to the AdpA-binding motif (TGGCCGGCCC versus TGGC SNGWWY, where S is G/C, W is A/T, and Y is T/C [57]) located 134 nt upstream of the α-*abeA* transcription start site (Fig. 5E). To determine whether the increased expression of α-*abeA* in the *rnc* (*absB*) mutant was mediated through AdpA, we created an *rnc adpA* double mutant and examined α-*abeA* expression. We found that α-*abeA* levels remained high in the double mutant strain (data not shown), suggesting that increased α-*abeA* transcription in the *rnc* mutant was not due to increased activation by AdpA but was instead mediated through RNase III by another, yet-to-be-determined mechanism.

DISCUSSION

Here, we elucidate the regulation of a novel gene cluster having a role in antibiotic production in *S. coelicolor*. On solid media, we showed that the overexpression of *abeABCD* and/or *abeR* resulted in the increased production of the blue-pigmented antibiotic actinorhodin, while the deletion of *abeR* resulted in decreased actinorhodin production. Unlike many genes that affect antibiotic production in *S. coelicolor* when overexpressed (e.g., *metK* [33] and *afsR* [15]), *abe* gene/cluster overexpression resulted in the maintenance of *actII-orf4* expression at elevated levels later in development rather than stimulating expression at all stages of culture growth.

Antibiotic production is subject to multiple levels of regulatory control and is impacted by physiological factors, like metabolic precursor concentrations, and by environmental conditions, like nutrient availability and signaling molecule abundance. Given the putative membrane localization of AbeB and AbeC and the cytoplasmic positioning of the TIR-like domain-containing AbeD, we considered the possibility that these proteins may have a role in sensing and responding to environmental cues. *S. coelicolor* produces at least three chromosomally encoded γ-butyrolactone signaling molecules, SCB1, SCB2, and SCB3 (20, 47), along with the plasmid-encoded methylenomycin furans (MMFs) (11, 34). However, these molecules all are freely diffusible across cytoplasmic membranes and bind dedicated cytoplasmic receptor proteins, making it unlikely that the *abe* proteins have an intermediary role in sensing or transducing signals in response to these molecules, although we cannot exclude the possibility that they recognize a currently unknown signaling molecule(s). We also considered the possibility that the *abe* gene cluster responds to changes in the nutritional status of the colony and/or influences the switch from primary to secondary metabolism, given that *abeBCD* and *abeR* expression initiated at a time consistent with this physiological transition. We also observed increased antibiotic production only on media where glucose was included as the primary carbon source (SMMS and R2YE), suggesting that the *abe* gene effect is subject to catabolite repression. Recent work has begun to illuminate the regulatory connections linking primary and secondary metabolism, with the regulators DasR and AtrA having central but antagonistic roles (37, 51). DasR negatively regulates actinorhodin and undecylprodigiosin production through the repression of *actII-orf4* and *redZ* (encoding a regulator of RedD expression); repression is relieved in the presence of *N*-acetylglucosamine (GlcNAc), although only during growth on poor carbon sources (37). AtrA directly activates the expression of *actII-orf4* and stimulates actinorhodin production but does not affect the production of undecylprodigiosin (51). It also activates the expression of *nagE2*, which encodes the permease specific for the import of GlcNAc into the cell (31a). There is no obvious connection between the *abe* genes and either DasR or AtrA: there are no binding sites for either protein upstream of *abeR*, the effect of *abe* gene overexpression does not require a poor carbon source, and *actII-orf4* expression during *abe* overexpression is not significantly altered, instead appearing to be extended during culture growth.

Both *abeR* and *abeABCD* overexpression enhanced actinorhodin production, but interestingly, the deletion of each did not have the same phenotypic consequences: the deletion of *abeR* significantly reduced actinorhodin production, while the loss of *abeABCD* had little effect on antibiotic levels. This suggested that AbeR has additional regulatory targets in the cell, or that AbeR has other functions in the cell that are independent of its transcriptional activator role (possibly mediated through its uncharacterized C-terminal domain). We defined the AbeR binding site through EMSA and DNase I footprinting experiments and found that, like other SARPs, AbeR bound heptameric direct repeats separated by 4 or 15 nt positioned on the same face of the DNA helix upstream of *abeBCD*. A search of the genome using the CGGAA(G/C)C $(n_{4/15})$CGGAA(G/C)C sequence as a query failed to identify other candidate binding sites. Thus, the only known AbeR binding sites are within the *abeA* coding sequence. It is interesting that most SARPs control the expression of genes that are located in close proximity on the chromosome.

The differential expression of genes within the *abeABCD* operon is not unprecedented in *S. coelicolor* (9), but it also is not considered to be the norm. Microarray studies of *S. coelicolor* gene expression have shown that the first gene of an operon is typically the most highly expressed, with expression levels then decreasing throughout the length of the operon (26). This is obviously not the case for *abeA*, which was expressed at far lower levels than any of the other *abe* genes. Comprehensive transcriptome analyses of *E. coli* (13, 41), *Helicobacter pylori* (43), *Listeria monocytogenes* (50), and *Mycoplasma pneumonia* (18) now are beginning to shed light on the transcriptional complexity that exists in bacteria. Recent studies of *H. pylori* and *M. pneumoniae* have revealed extensive intraoperon expression dynamics, with different genes within an operon having distinct induction/repression characteristics relative to other genes within the same operon. Our findings here are consistent with there being flexible operon expression in *S. coelicolor*. Additional complexity at the antisense transcript level also is appearing to be widespread, with antisense transcripts being detected throughout the *E. coli*, *H. pylori*, and *M. pneumonia* genomes (13, 18, 41, 43). What role these antisense transcripts have in regulating gene expression or protein activity remains to be seen.

Unexpectedly, we found that α-*abeA* did not appear to have a role in modulating the transcript stability of its sense counterpart, *abeA*, as increased levels of α-*abeA* in an *rnc* (*absB*)

mutant could not be correlated with a subsequent change in *abeA* transcript abundance. While we cannot exclude the possibility that α-*abeA* controls *abeA* expression via an RNase III-independent mechanism (e.g., *abeA* translation), we did observe changes in the overall transcript abundance of both *abeA* and α-*abeA* when RNase III was absent. *abeA* transcripts, as well as *abeBCD* transcripts, were consistently less abundant in an *rnc* (*absB*) mutant than in its wild-type parent. This is reminiscent of the reduced expression seen for the antibiotic biosynthetic clusters of actinorhodin, undecylprodigiosin, CDA, and a cryptic polyketide in an *absB* mutant (21). In contrast, α-*abeA* levels were increased in the *rnc* (*absB*) knockout strain. This effect was not mediated through AdpA, which is negatively regulated by RNase III, and may instead reflect either the direct targeting of α-*abeA* by RNase III during later growth stages or control by some other RNase III-dependent factor.

ACKNOWLEDGMENTS

We thank David Capstick, Henry Haiser, and Justin Nodwell for the critical reading of the manuscript and for helpful comments and suggestions and Ye Xu and Justin Nodwell for the use of their reporter plasmids.

This work was funded by grants from the Natural Sciences and Engineering Research Council of Canada (NSERC Discovery Grant no. 312495 and NSERC Collaborative Research and Development Grant no. 335144), the Canada Research Chairs (CRC) program, and graduate student awards from the Province of Ontario (to H.) and NSERC (to P.P.).

REFERENCES

1. **Aceti, D. J., and W. C. Champness.** 1998. Transcriptional regulation of *Streptomyces coelicolor* pathway-specific antibiotic regulators by the *absA* and *absB* loci. J. Bacteriol. **180:**3100–3106.
2. **Arias, P., M. A. Fernández-Moreno, and F. Malpartida.** 1999. Characterization of the pathway-specific positive transcriptional regulator for actinorhodin biosynthesis in *Streptomyces coelicolor* A3(2) as a DNA-binding protein. J. Bacteriol. **181:**6958–6968.
3. **Bentley, S. D., K. F. Chater, A. M. Cerdeño-Tarraga, G. L. Challis, N. R. Thomson, K. D. James, D. E. Harris, M. A. Quail, H. Kieser, D. Harper, A. Bateman, S. Brown, G. Chandra, C. W. Chen, M. Collins, A. Cronin, A. Fraser, A. Goble, J. Hidalgo, T. Hornsby, S. Howarth, C. H. Huang, T. Kieser, L. Larke, L. Murphy, K. Oliver, S. O'Neil, E. Rabbinowitsch, M. A. Rajandream, K. Rutherford, S. Rutter, K. Seeger, D. Saunders, S. Sharp, R. Squares, S. Squares, K. Taylor, T. Warren, A. Wietzorrek, J. Woodward, B. G. Barrell, J. Parkhill, and D. A. Hopwood.** 2002. Complete genome sequence of the model actinomycete *Streptomyces coelicolor* A3(2). Nature **417:**141–147.
4. **Bibb, M. J.** 1996. The regulation of antibiotic production in *Streptomyces coelicolor* A3(2). Microbiology **142:**1335–1344.
5. **Bibb, M. J.** 2005. Regulation of secondary metabolism in streptomycetes. Curr. Opin. Microbiol. **8:**208–215.
6. **Bradford, M. M.** 1976. A rapid and sensitive method for the quantitation of microgram quantities of protein utilizing the principle of protein-dye binding. Anal. Biochem. **72:**248–254.
7. **Capstick, D. S., J. M. Willey, M. J. Buttner, and M. A. Elliot.** 2007. SapB and the chaplins: connections between morphogenetic proteins in *Streptomyces coelicolor*. Mol. Microbiol. **64:**602–613.
8. **Chakraburtty, R., and M. Bibb.** 1997. The ppGpp synthetase gene (*relA*) of *Streptomyces coelicolor* A3(2) plays a conditional role in antibiotic production and morphological differentiation. J. Bacteriol. **179:**5854–5861.
9. **Charaniya, S., S. Mehra, W. Lian, K. P. Jayapal, G. Karypis, and W. S. Hu.** 2007. Transcriptome dynamics-based operon prediction and verification in *Streptomyces coelicolor*. Nucleic Acids Res. **35:**7222–7236.
10. **Chater, K. F.** 2006. *Streptomyces* inside-out: a new perspective on the bacteria that provide us with antibiotics. Philos. Trans. R. Soc. B Biol. Sci. **361:**761–768.
11. **Corre, C., L. Song, S. O'Rourke, K. F. Chater, and G. L. Challis.** 2008. 2-Alkyl-4-hydroxymethylfuran-3-carboxylic acids, antibiotic production inducers discovered by *Streptomyces coelicolor* genome mining. Proc. Natl. Acad. Sci. U. S. A. **105:**17510–17515.
12. **Craney, A., T. Hohenauer, Y. Xu, N. K. Navani, Y. Li, and J. Nodwell.** 2007. A synthetic *luxCDABE* gene cluster optimized for expression in high-GC bacteria. Nucleic Acids Res. **35:**e46.
13. **Dornenburg, J. E., A. M. DeVita, M. J. Palumbo, and J. T. Wade.** 2010. Widespread antisense transcription in *Escherichia coli*. mBio **1:**e00024–10.
14. **Elliot, M. A., N. Karoonuthaisiri, J. Huang, M. J. Bibb, S. N. Cohen, C. M. Kao, and M. J. Buttner.** 2003. The chaplins: a family of hydrophobic cell-surface proteins involved in aerial mycelium formation in *Streptomyces coelicolor*. Genes Dev. **17:**1727–1740.
15. **Floriano, B., and M. Bibb.** 1996. *afsR* is a pleiotropic but conditionally required regulatory gene for antibiotic production in *Streptomyces coelicolor* A3(2). Mol. Microbiol. **21:**385–396.
16. **Gravenbeek, M. L., and G. H. Jones.** 2008. The endonuclease activity of RNase III is required for the regulation of antibiotic production by *Streptomyces coelicolor*. Microbiology **154:**3547–3555.
17. **Gregory, M. A., R. Till, and M. C. M. Smith.** 2003. Integration site for *Streptomyces* phage phiBT1 and development of site-specific integrating vectors. J. Bacteriol. **185:**5320–5323.
18. **Güell, M., V. van Noort, E. Yus, W. H. Chen, J. Leigh-Bell, K. Michalodimitrakis, T. Yamada, M. Arumugam, T. Doerks, S. Kühner, M. Rode, M. Suyama, S. Schmidt, A. C. Gavin, P. Bork, and L. Serrano.** 2009. Transcriptome complexity in a genome-reduced bacterium. Science **326:**1268–1271.
19. **Gust, B., G. L. Challis, K. Fowler, T. Kieser, and K. F. Chater.** 2003. PCR-targeted *Streptomyces* gene replacement identifies a protein domain needed for biosynthesis of the sesquiterpene soil odor geosmin. Proc. Natl. Acad. Sci. U. S. A. **100:**1541–1546.
20. **Hsiao, N. H., S. Nakayama, M. E. Merlo, M. de Vries, R. Bunet, S. Kitani, T. Nihira, and E. Takano.** 2009. Analysis of two additional signaling molecules in *Streptomyces coelicolor* and the development of a butyrolactone-specific reporter system. Chem. Biol. **16:**951–960.
21. **Huang, J., J. Shi, V. Molle, B. Sohlberg, D. Weaver, M. J. Bibb, N. Karoonuthaisiri, C.-J. Lih, C. M. Kao, M. J. Buttner, and S. N. Cohen.** 2005. Cross-regulation among disparate antibiotic biosynthetic pathways of *Streptomyces coelicolor*. Mol. Microbiol. **58:**1276–1287.
22. **Janssen, G. R., and M. J. Bibb.** 1993. Derivatives of pUC18 that have BglII sites flanking a modified multiple cloning site and that retain the ability to identify recombinant clones by visual screening of *Escherichia coli* colonies. Gene **124:**133–134.
23. **Kang, S. G., W. Jin, M. J. Bibb, and K. J. Lee.** 1998. Actinorhodin and undecylprodigiosin production in wild-type and *relA* mutant strains of *Streptomyces coelicolor* A3(2) grown in continuous culture. FEMS Microbiol. Lett. **168:**221–226.
24. **Kieser, T., M. J. Bibb, M. J. Buttner, K. F. Chater, and D. A. Hopwood.** 2000. Practical *Streptomyces* genetics. John Innes Foundation, Norwich, United Kingdom.
25. **Kim, D. W., K. Chater, K. J. Lee, and A. Hesketh.** 2005. Changes in the extracellular proteome caused by the absence of the *bldA* gene product, a developmentally significant tRNA, reveal a new target for the pleiotropic regulator AdpA in *Streptomyces coelicolor*. J. Bacteriol. **187:**2957–2966.
26. **Laing, E., V. Mersinias, C. Smith, and S. Hubbard.** 2006. Analysis of gene expression in operons of *Streptomyces coelicolor*. Genome Biol. **7:**R46.
27. **Le, T. B. K., H. P. Fiedler, C. D. den Hengst, S. K. Ahn, A. Maxwell, and M. J. Buttner.** 2009. Coupling of the biosynthesis and export of the DNA gyrase inhibitor simocyclinone in *Streptomyces antibioticus*. Mol. Microbiol. **72:**1462–1474.
28. **MacNeil, D. J., K. M. Gewain, C. L. Ruby, G. Dezeny, P. H. Gibbons, and T. MacNeil.** 1992. Analysis of *Streptomyces avermitilis* genes required for avermectin biosynthesis utilizing a novel integration vector. Gene **111:**61–68.
29. **Malpartida, F., and D. A. Hopwood.** 1986. Physical and genetic characterisation of the gene cluster for the antibiotic actinorhodin in *Streptomyces coelicolor* A3(2). Mol. Gen. Genet. **205:**66–73.
30. **Martin, M. U., and H. Wesche.** 2002. Summary and comparison of the signaling mechanisms of the Toll/interleukin-1 receptor family. Biochim. Biophys. Acta Mol. Cell Res. **1592:**265–280.
31. **Martínez-Hackert, E., and A. M. Stock.** 1997. The DNA-binding domain of OmpR: crystal structures of a winged helix transcription factor. Structure **5:**109–124.

31a. **Nothaft, H., S. Rigali, B. Boomsma, M. Swiatek, K. J. McDowall, G. P. van Wezel, and F. Titgemeyer.** 2010. The permease gene *nagE2* is the key to *N*-acetylglucosamine sensing and utilization in *Streptomyces coelicolor* and is subject to multi-level control. Mol. Microbiol. **75:**1133–1144.

32. **Ohnishi, Y., S. Kameyama, H. Onaka, and S. Horinouchi.** 1999. The A-factor regulatory cascade leading to streptomycin biosynthesis in *Streptomyces griseus*: identification of a target gene of the A-factor receptor. Mol. Microbiol. **34:**102–111.
33. **Okamoto, S., A. Lezhava, T. Hosaka, Y. Okamoto-Hosoya, and K. Ochi.** 2003. Enhanced expression of S-adenosylmethionine synthetase causes overproduction of actinorhodin in *Streptomyces coelicolor* A3(2). J. Bacteriol. **185:**601–609.
34. **O'Rourke, S., A. Wietzorrek, K. Fowler, C. Corre, G. L. Challis, and K. F. Chater.** 2009. Extracellular signalling, translational control, two repressors and an activator all contribute to the regulation of methylenomycin production in *Streptomyces coelicolor*. Mol. Microbiol. **71:**763–778.
35. **Price, B., T. Adamidis, R. Kong, and W. Champness.** 1999. A *Streptomyces*

coelicolor antibiotic regulatory gene, *absB*, encodes an RNase III homolog. J. Bacteriol. **181:**6142–6151.
36. **Redenbach, M., H. M. Kieser, D. Denapaite, A. Eichner, J. Cullum, H. Kinashi, and D. A. Hopwood.** 1996. A set of ordered cosmids and a detailed genetic and physical map for the 8 Mb *Streptomyces coelicolor* A3(2) chromosome. Mol. Microbiol. **21:**76–96.
37. **Rigali, S., F. Titgemeyer, S. Barends, S. Mulder, A. W. Thomae, D. A. Hopwood, and G. P. van Wezel.** 2008. Feast or famine: the global regulator DasR links nutrient stress to antibiotic production by *Streptomyces*. EMBO Rep. **9:**670–675.
38. **Sambrook, J., and D. W. Russell.** 2001. Molecular cloning: a laboratory manual, 3rd ed. Cold Spring Harbor Laboratory Press, Cold Spring Harbor, NY.
39. **Santos-Beneit, F., A. Rodríguez-Garcia, A. Sola-Landa, and J. F. Martín.** 2009. Cross-talk between two global regulators in *Streptomyces*: PhoP and AfsR interact in the control of *afsS*, *pstS* and *phoRP* transcription. Mol. Microbiol. **72:**53–68.
40. **Sekurova, O. N., T. Brautaset, H. Sletta, S. E. F. Borgos, Ø. M. Jakobsen, T. E. Ellingsen, A. R. Strøm, S. Valla, and S. B. Zotchev.** 2004. In vivo analysis of the regulatory genes in the nystatin biosynthetic gene cluster of *Streptomyces noursei* ATCC 11455 reveals their differential control over antibiotic biosynthesis. J. Bacteriol. **186:**1345–1354.
41. **Selinger, D. W., K. J. Cheung, R. Mei, E. M. Johansson, C. S. Richmond, F. R. Blattner, D. J. Lockhart, and G. M. Church.** 2000. RNA expression analysis using a 30 base pair resolution *Escherichia coli* genome array. Nat. Biotechol. **18:**1262–1268.
42. **Sello, J. K., and M. J. Buttner.** 2008. The gene encoding RNase III in *Streptomyces coelicolor* is transcribed during exponential phase and is required for antibiotic production and for proper sporulation. J. Bacteriol. **190:**4079–4083.
43. **Sharma, C. M., S. Hoffmann, F. Darfeuille, J. Reignier, S. Findeisz, A. Sittka, S. Chabas, K. Reiche, J. Hackermuller, R. Reinhardt, P. F. Stadler, and J. Vogel.** 2010. The primary transcriptome of the major human pathogen *Helicobacter pylori*. Nature **464:**250–255.
44. **Spear, A. M., N. J. Loman, H. S. Atkins, and M. J. Pallen.** 2009. Microbial TIR domains: not necessarily agents of subversion? Trends Microbiol. **17:**393–398.
45. **Swiercz, J., P. Hindra, J. Bobek, H. J. Haiser, C. Di Berardo, B. Tjaden, and M. A. Elliot.** 2008. Small noncoding RNAs in *Streptomyces coelicolor*. Nucleic Acids Res. **36:**7240–7251.
46. **Tahlan, K., S. K. Ahn, A. Sing, T. D. Bodnaruk, A. R. Willems, A. R. Davidson, and J. R. Nodwell.** 2007. Initiation of actinorhodin export in *Streptomyces coelicolor*. Mol. Microbiol. **64:**951–961.
47. **Takano, E.** 2006. γ-Butyrolactones: *Streptomyces* signalling molecules regulating antibiotic production and differentiation. Curr. Opin. Microbiol. **9:**287–294.
48. **Takano, E., H. C. Gramajo, E. Strauch, N. Andres, J. White, and M. J. Bibb.** 1992. Transcriptional regulation of the *redD* transcriptional activator gene accounts for growth-phase-dependent production of the antibiotic undecylprodigiosin in *Streptomyces coelicolor* A3(2). Mol. Microbiol. **6:**2797–2804.
49. **Tanaka, A., Y. Takano, Y. Ohnishi, and S. Horinouchi.** 2007. AfsR recruits RNA polymerase to the *afsS* promoter: a model for transcriptional activation by SARPs. J. Mol. Biol. **369:**322–333.
50. **Toledo-Arana, A., O. Dussurget, G. Nikitas, N. Sesto, H. Guet-Revillet, D. Balestrino, E. Loh, J. Gripenland, T. Tiensuu, K. Vaitkevicius, M. Barthelemy, M. Vergassola, M. A. Nahori, G. Soubigou, B. Régnault, J. Y. Coppée, M. Lecuit, J. Johansson, and P. Cossart.** 2009. The *Listeria* transcriptional landscape from saprophytism to virulence. Nature **459:**950–956.
51. **Uguru, G. C., K. E. Stephens, J. A. Stead, J. E. Towle, S. Baumberg, and K. J. McDowall.** 2005. Transcriptional activation of the pathway-specific regulator of the actinorhodin biosynthetic genes in *Streptomyces coelicolor*. Mol. Microbiol. **58:**131–150.
52. **Vara, J., M. Lewandowska-Skarbek, Y. G. Wang, S. Donadio, and C. R. Hutchinson.** 1989. Cloning of genes governing the deoxysugar portion of the erythromycin biosynthesis pathway in *Saccharopolyspora erythraea* (*Streptomyces erythreus*). J. Bacteriol. **171:**5872–5881.
53. **Vogtli, M., P. C. Chang, and S. N. Cohen.** 1994. *afsR2*: a previously undetected gene encoding a 63-amino-acid protein that stimulates antibiotic production in *Streptomyces lividans*. Mol. Microbiol. **14:**643–653.
54. **Wietzorrek, A., and M. Bibb.** 1997. A novel family of proteins that regulates antibiotic production in streptomycetes appears to contain an OmpR-like DNA-binding fold. Mol. Microbiol. **25:**1181–1184.
55. **Wilson, D. J., Y. Xue, K. A. Reynolds, and D. H. Sherman.** 2001. Characterization and analysis of the PikD regulatory factor in the pikromycin biosynthetic pathway of *Streptomyces venezuelae*. J. Bacteriol. **183:**3468–3475.
56. **Xu, W., J. Huang, R. Lin, J. Shi, and S. N. Cohen.** 2010. Regulation of morphological differentiation in *S. coelicolor* by RNase III (AbsB) cleavage of mRNA encoding the AdpA transcription factor. Mol. Microbiol. **75:**781–791.
57. **Yamazaki, H., A. Tomono, Y. Ohnishi, and S. Horinouchi.** 2004. DNA-binding specificity of AdpA, a transcriptional activator in the A-factor regulatory cascade in *Streptomyces griseus*. Mol. Microbiol. **53:**555–572.
58. **Yeats, C., S. Bentley, and A. Bateman.** 2003. New knowledge from old: *in silico* discovery of novel protein domains in *Streptomyces coelicolor.* BMC Microbiol. doi:10.1186/1471-2180-3-3.